Top Surface Layer Sensitivity in Proton-Induced Auger Electron Spectroscopy

R. Pfandzelter and J. Landskron
Sektion Physik, Universität München, Amalienstrasse 54, 8000 München 40, Germany
(Received 21 September 1992)

We report on a new technique, Auger electron spectroscopy induced by impact of specularly reflected energetic protons. The Cu $M_{2,3}VV$ Auger signal induced by 175 keV protons incident on clean and Ag-covered Cu(111) is measured. At 0.5° incidence angle, a coverage of 1 monolayer produces a reduction in Auger signal to merely 2% of the clean-surface signal. This is far less than for electron or large-angle proton excitation (37%). The extreme reduction is due to the fact that the grazingly incident protons are specularly reflected and solely create core holes at top surface layer atoms.

PACS numbers: 61.80.Jh, 68.35.−p, 79.20.Rf

Auger electron spectroscopy (AES) is a most powerful and widely used analysis technique in surface physics and surface chemistry. It has been profitably exploited to investigate electronic, magnetic, chemical, and structural properties of surfaces and thin films. Usually Auger electrons are induced by electrons with beam energies of a few keV and normal-to-surface or oblique incidence. Proton-induced AES with beam energies of some hundred keV essentially provides the same information, but is far less common due to the higher complexity in apparatus. The main advantage over electron-induced AES is that energetic protons suffer only little energy loss and angular deflection in the near-surface region, whereas the strong scattering of primary electrons causes considerable uncertainty in the depth distribution of generated Auger electrons. In both cases, however, the generation depths usually surpass the escape depths of the lower energetic Auger electrons by far. The escape depths are determined by the hot-electron transport properties in solids and vary between several Å and several tens of Å in the range of principal Auger electron energies and normal-to-surface exit [1]. Thus, a limited surface sensitivity is inherently involved in conventional AES; even in the optimum case of some 10 eV Auger electron energies, several layers beneath a surface are sampled simultaneously. For numerous applications this is not sufficient and a sensitivity to the top surface layer is highly desired.

The surface sensitivity of AES can be enhanced by using collection angles off the surface normal [2]. Yet in order to obtain considerable improvement, rather small angles have to be used, since the escape depth as a function of angle is roughly described by a cosine function [1]. Whether a sensitivity to the top surface layer may be achieved by using grazing collection angles has not been addressed so far. The other way to enhance surface sensitivity consists of changing the depth distribution function of the Auger electron generation. This has been achieved to a high degree by positron-annihilation-induced AES [3]: Low-energy positrons became trapped in a surface state and create core holes by matter-antimatter annihilation. At present, this technique suffers from the low positron beam currents available. Beyond that, only low-energy Auger electrons are generated due to the rapidly decreasing annihilation probability with decreasing electron orbit radius. Another exciting possibility is offered by proton-induced AES: Energetic protons which are grazingly incident upon a flat surface do not penetrate into the surface, but are specularly reflected at the planar surface potential. The trajectories thus clearly deviate from the (essentially) straight-line trajectories at larger incident angles, which give rise to a uniform-in-depth Auger electron generation. In grazing-angle proton-surface scattering, however, only Auger electrons from top surface layer atoms should be induced. This most promising concept has been recently proposed and tested at clean crystal surfaces by Pfandzelter and Lee [4] and Rau *et al.* [5]. The experiments, however, cannot prove whether top surface layer sensitivity is actually achieved.

In this Letter, we report on an overlayer experiment to check the applicability and surface sensitivity of proton-induced AES at grazing angles and to give advice for a proper selection of incidence angles, which, as we shall see, is of pivotal importance. The basic idea is quite simple: A flat crystal surface is covered by 1 monolayer of a different material; if top surface layer sensitivity is obtained, no more substrate Auger electrons should be detected. As the overlayer/substrate system we choose Ag on Cu(111). This system has been thoroughly studied by different groups using a variety of techniques. Silver and copper are almost immiscible and interdiffusion occurs only at high temperature [6,7]; the growth mode follows the layer-by-layer mode up to at least 4 monolayers of silver [8–12]. We can thus expect 1 monolayer (ML) of Ag deposited on Cu(111) to provide a continuous and atomically flat overlayer covering the topmost copper surface layer. In addition, the Cu $M_{2,3}VV$ Auger transition at 61 eV provides a crucial test for an aspired improvement in surface sensitivity, since in this range of Auger electron energies the surface sensitivity is already maximal in conventional AES.

The copper single crystal (12 mm diam) was polished and carefully oriented to a residual deviation from the (111) face of less than 10′. The surface was cleaned *in* *situ* by cycles of mild sputtering (600 eV Ar^+, 5 $\mu A/cm^2$, 5 min) and subsequent annealing (820 K, 10 min), until no more contamination was detected by AES, and LEED showed sharp diffraction spots. High purity silver (99.9999%) was deposited by evaporation from a molybdenum crucible warmed by the Joule effect. The amount of Ag deposited was monitored by means of an oscillating quartz, calibrated beforehand by a second oscillating quartz mounted exactly at the target position. In proton-induced AES, a mass-selected, monoenergetic beam of 175 keV H^+ is incident to the target surface at a grazing angle Φ with a current density of 20 nA/mm^2 and a maximum divergence of $\pm 0.07°$. The adjustment of the incidence angle Φ is monitored by a laser beam with an accuracy of $\pm 0.05°$. Electron-induced AES is performed using a 1.5 keV electron beam at normal incidence with a current density of some 100 nA/mm^2. A single-pass cylindrical mirror analyzer (CMA) collects Auger electrons emitted at an angle of about $48° \pm 6°$ to the surface over the full 360° cone. In electron-induced AES, the relative energy resolution amounts to 2.6% FWHM; it is somewhat worse in proton-induced AES due to the finite source size at glancing incidence. Computerized pulse counting detection is applied with an electron pass energy step width of 0.36 eV and an accumulation time of 500 ms per step. No numerical processing of the Auger electron spectra is used apart from division by the pass energy to account for the constant relative energy resolution. The substrate position is the same for silver deposition and AES data collection, i.e., adjustment errors are minimized; during the AES measurements, deposition is interrupted by a shutter. The rate of deposition is 0.1 ML/min; the substrate temperature is about 400 K. The base pressure in the UHV chamber is 3×10^{-10} mbar.

First of all, we measured the *electron*-induced Cu Auger signal S_A as a function of the Ag coverage Θ. The Auger signal is obtained by electron background subtraction from the measured $N(E)$ spectra followed by integration. The background is approximated by spline interpolation under the Auger peak from the low- and high-energy portions of each spectrum. [For comparison, other, more sophisticated methods of background removal (e.g., convolution technique [13]) have been tested. Though the Auger signal is slightly smaller than the corresponding spline-retrieved Auger signal due to proper elimination of inelastically scattered Auger electrons, the normalized S_A-Θ plots are identical within the experimental error.] Figure 1 shows the Auger signal normalized to the clean-surface value versus coverage. The plot forms straight lines with different gradients as expected for growth in a layer-by-layer fashion [14]. The sharp break point indicates the completion of the first monolayer; the monolayer density has been determined to $(1.50\pm 0.15)\times 10^{15}$ $atoms/cm^2$. At 1 ML the Auger signal has decreased to $(37\pm 2)\%$ of the clean-surface signal. This shows that second and deeper atomic layers contribute considerably to the observed Auger signal in electron-induced AES even for Auger transitions with inherently high surface sensitivity. In case of not too small incidence angles, this should apply to *proton*-induced AES as well. Figure 2(a) shows the proton-induced Auger signal versus coverage for an incidence angle $\Phi = 4.0°$. Again, albeit with some uncertainty due to the larger scatter in the data, the plot forms straight lines with roughly the same gradients and break point position [$S_A = (37\pm 5)\%$ for $\Theta = 1$ ML], i.e., the same number of atomic layers beneath the surface is probed. This, however, changes for grazing incidence angles. For $\Phi = 1.0°$ [Fig. 2(b)], the Auger signal has decreased to about 25% for 1 monolayer, because specular reflection gradually evolves in the neighborhood of the critical angle $\Phi_s = 1.2°$ [15], i.e., part of the protons are reflected at the top surface layer and the surface sensitivity of AES is determined by the generation depth distribution rather than the escape depth of the Auger electrons. In addition to the rapid decrease of the Auger signal in the submonolayer coverage regime, a deviation from the linear behavior is observed. This is not surprising, since each proton that undergoes specular reflection interacts with numerous surface layer atoms along its trajectory, i.e., the S_A-Θ plot crucially depends on the size and spatial distributions of the growing islands. In order to elucidate this dependence, computer simulations have to be performed; a simple and general description of the scattering process using planar potentials is only possible when a complete monolayer is formed.

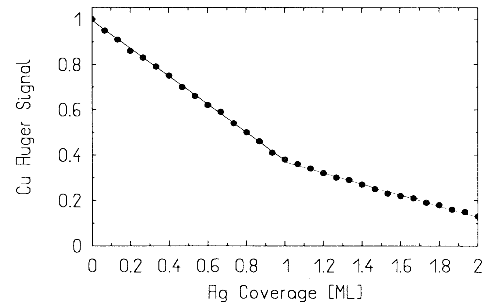

FIG. 1. Cu $M_{2,3}VV$ Auger signal vs Ag coverage. The Auger electrons are induced by a 1.5 keV electron beam at normal incidence. The straight lines are the results of least-squares fits to the data below and beyond 1 ML, respectively.

The findings at $\Phi = 1.0°$ are more pronounced for still smaller incidence angles. At $\Phi = 0.8°$ [Fig. 2(c)], $S_A = 15\%$ for $\Theta = 1$ ML and roughly constant for larger Θ. Finally, at $\Phi = 0.5°$ [Fig. 2(d)], the Auger signal for 1 monolayer has decreased to merely 2%, i.e., 1 monolayer of Ag on Cu(111) is enough to completely prevent a generation of Cu Auger electrons. Because the planar potentials of 1 monolayer of Ag atoms on Cu(111) and a clean Cu(111) surface layer are almost equal [15], we thus

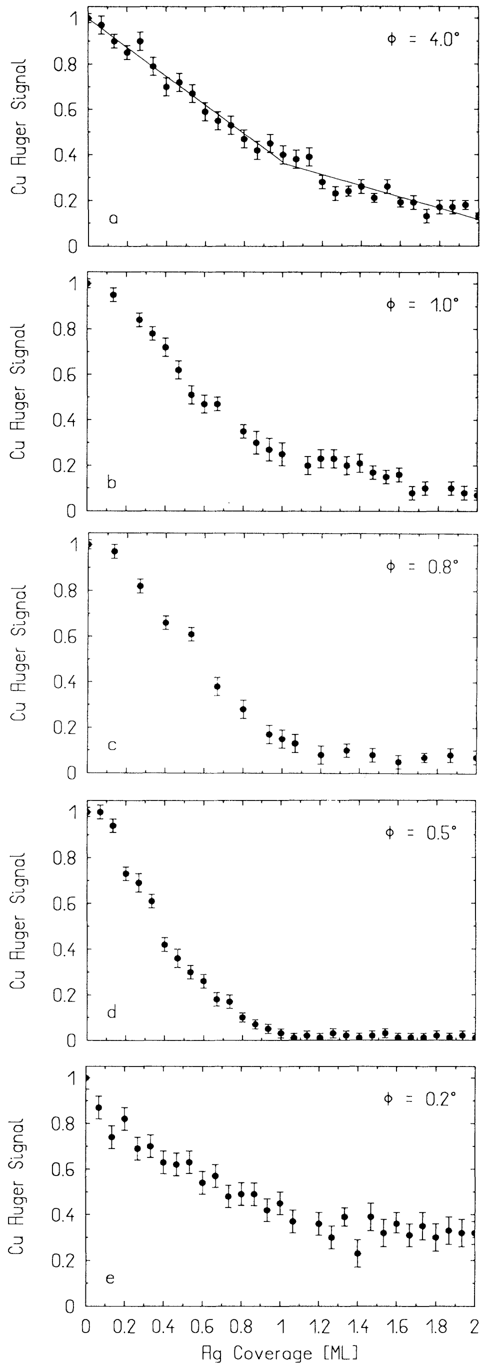

FIG. 2. Cu $M_{2,3}VV$ Auger signal vs Ag coverage. The Auger electrons are induced by a 175 keV proton beam incident at an angle Φ to the surface plane as indicated. The straight lines in (a) are the results of least-squares fits to the data below and beyond 1 ML, respectively.

conclude that the Cu Auger signal at the clean surface for $\Phi=0.5°$ originates almost exclusively (98%) from top surface layer atoms.

The trajectory in specular reflection and thus the closest distance d_{min} of the protons towards the clean Cu(111) surface can be easily calculated by using appropriate potentials. For $\Phi=0.5°$, d_{min} amounts to 0.9 Å [15]. This is not much larger than the Bohr adiabatic distance for core-hole excitation in the $M_{2,3}$ shell, $d_{ad}=0.5$ Å, which thus enables Cu $M_{2,3}VV$ Auger electron generation by specularly reflected protons. For $d_{min} \gg d_{ad}$, however, Auger electron generation should decrease considerably. Actually, this is observed by further reducing the incidence angle to $\Phi=0.2°$. Here d_{min} amounts to 1.9 Å and the Auger signal for the clean surface has decreased to only about 20% of the value at $\Phi=0.5°$. The corresponding S_A-Θ plot is shown in Fig. 2(e). It closely resembles, at least in the submonolayer coverage regime, the electron-induced S_A-Θ plot (cf. Fig. 1). The explanation is thus obvious: Some of the protons penetrate inside the crystal via defects at the surface (e.g., steps) and thus give rise to a (more or less) uniform-in-depth Auger electron generation. Though this happens for larger incidence angles as well, it is more likely to occur at the smallest angles due to the larger interaction lengths. Most important, however, is that the competing process of Auger electron generation by specularly reflected protons is hardly effective here.

In summary, the overlayer experiment presented here gives clear evidence that protons which are incident at a suitably chosen grazing angle upon a flat crystal surface selectively induce Auger electrons at top surface layer atoms. As regards the proper choice of incidence angles, the requirements that have to be met are twofold. First, the incidence angle must be *small* enough to ensure specular reflection. Second, the angle must be *large* enough to allow appreciable core-hole excitations, i.e., the distance of closest approach towards the surface must not exceed the adiabatic distance substantially. We note that for any surface and any Auger transition (even high-energy transitions), a proper range of incidence angles can be found by simply adjusting the proton beam energy. The combination of proton-induced AES and specular reflection thus provides a new and unique means to get many kinds of information accessible to conventional AES, but solely from the top surface layer. The crucial prerequisite, however, are specimens that are sufficiently flat, which restricts the applicability of the technique to smooth crystal surfaces with terrace widths that exceed the interaction length of the protons with the surface. An exciting prospect is the investigation of the local electronic structure at the very surface (e.g., core-hole screening, electron-electron correlation) by means of an Auger line shape analysis. Here, the technique also profits by the lack of backscattered electrons and, more important, the considerable decrease of electron energy-loss processes, which mitigates the background problem with respect to signal retrieval and should enable direct recording of the intrinsic energetic shape of Auger peaks. In addition, the method should give valuable information about growth mode and initial nucleation of thin films by measuring the

Auger signal versus coverage, since the protons' trajectories are well defined and can be easily calculated by computer simulation for different film topographies. In the case of well-known clean crystal surfaces, the method may be profitably exploited to study the impact parameter dependence of core-hole excitation probabilities.

This work was funded by the German Federal Minister for Research and Technology (BMFT) under Contract No. 03SI3LMU.

[1] J. Ferrón and E. C. Goldberg, Surf. Sci. **275**, 114 (1992).
[2] G. B. Hoflund, D. A. Asbury, C. F. Corallo, and G. R. Corallo, J. Vac. Sci. Technol. A **6**, 70 (1988); M. R. Davidson, G. B. Hoflund, and R. A. Outlaw, J. Vac. Sci. Technol. A **9**, 1344 (1991).
[3] D. Mehl, A. R. Köymen, K. O. Jensen, F. Gotwald, and A. Weiss, Phys. Rev. B **41**, 799 (1990); K. H. Lee, A. R. Koymen, D. Mehl, K. O. Jensen, and A. Weiss, Surf. Sci. **264**, 127 (1992).
[4] R. Pfandzelter and J. W. Lee, Nucl. Instrum. Methods Phys. Res., Sect. B **45**, 641 (1990); J. W. Lee and R. Pfandzelter, Surf. Sci. **225**, 301 (1990).
[5] C. Rau and K. Waters, Nucl. Instrum. Methods Phys. Res., Sect. B **40/41**, 127 (1989); C. Rau, K. Waters, and N. Chen, Phys. Rev. Lett. **64**, 1441 (1990).
[6] M. Murakami and D. deFontaine, J. Appl. Phys. **47**, 2857 (1976).
[7] G. Gladyszewski and Z. Mitura, Surf. Sci. **231**, 90 (1990).
[8] M. J. Gibson and P. J. Dobson, J. Phys. F **5**, 1828 (1975).
[9] E. Bauer, Appl. Surf. Sci. **11/12**, 479 (1982).
[10] A. P. Shapiro, A. L. Wachs, and T.-C. Chiang, Solid State Commun. **58**, 121 (1986).
[11] Y. Borensztein, Europhys. Lett. **4**, 723 (1987).
[12] R. Pfandzelter and J. Landskron (to be published).
[13] N. Rosenberg, M. Tholomier, and E. Vicario, J. Electron Spectrosc. Relat. Phenom. **46**, 331 (1988).
[14] C. Argile and G. E. Rhead, Surf. Sci. Rep. **10**, 277 (1989).
[15] The planar potential is derived from a superposition of Thomas-Fermi-Molière potentials; the critical angle for specular reflection is calculated from the value of the planar potential at the Thomas-Fermi distance.